International Journal of Electrical Engineering and Technology (IJEET)
Volume 11, Issue 8, October 2020, pp. 127-133, Article ID: IJEET_11_08_012
Available online at https://iaeme.com/Home/issue/IJEET?Volume=11&Issue=10
ISSN Print: 0976-6545 and ISSN Online: 0976-6553
https://doi.org/10.34218/IJEET.11.8.2020.012

STUDY OF ELECTRICAL PROPERTIES OF IRON (III) OXIDE (FE_2O_3) NANOPOWDER BY IMPEDANCE SPECTROSCOPY

Chandra Kumar Dixit and Kapil Pandey
Department of Physics, Dr. Shakuntala Misra National Rehabilitation University, Lucknow (226017), India

ABSTRACT

The electrical properties of Iron (iii) Oxide (Fe_2O_3) were investigated by impedance spectroscopy over the frequency1 Hz to 10 MHz at room temperature. Scanning electron Microscopy (SEM) and Raman Spectroscopy has been done of Iron (iii) Oxide Nanopowder ranging 30-40 nm in diameter. The morphological analysis of Iron (iii) Oxide (Fe_2O_3) has been done by (SEM) informing the identical particles and diameters ranging 30-40 nm. Additional, the Raman shift deviation exhibit reliable peak found at ≈143, 289, 498 and 629 cm^{-1} of Iron (iii) Oxide (Fe_2O_3) Nanopowder. The electrical studies of the Iron (iii) Oxide (Fe_2O_3) Nanopowder have been inspected in order to obtain the dependency of electrical parameters (mainly dielectric permittivity, loss, conductivity, loss-tangent, impedance, and admittance) on frequency. Considerable dependency of the conductivity on frequency which is achieved owing to significant change in particle diameter. It calculated that the electrical parameters of Iron (iii) Oxide (Fe_2O_3) Nanopowder have a great dependency on the frequency.

Keywords: Fe_2O_3; SEM; Raman spectroscopy; Loss tangent; Electrical Conductivity

Cite this Article: Chandra Kumar Dixit and Kapil Pandey, Study of Electrical Properties of Iron (III) Oxide (FE_2O_3) Nanopowder by Impedance Spectroscopy, *International Journal of Electrical Engineering and Technology (IJEET)*, 11(8), 2020, pp. 127-133.
https://iaeme.com/Home/issue/IJEET?Volume=11&Issue=10

1. INTRODUCTION

From a very long time nanoparticles of iron oxides show exclusive and valuable characteristics for a number of applications. Among other Iron (iii) Oxide is one of the most versatile ferromagnetic materials with a high saturation magnetization, a Curie temperature well above the ambient, a relatively weak magneto-crystalline anisotropy and superparamagnetic behaviour in the fine particle state.[1-2] Nowadays, MNPs of the iron oxides have become important components in biosensing, magnetic separation, advanced medical screening and therapies, including bio-assays, magnetic resonance imaging (MRI), magnetically guided drug delivery, and hyperthermia, etc.[3-7] magnetite MNPs were also used in many other

applications such as storage media for magnetic memories, ferrofluids, magnetic separation, and catalysis.[4]

In the modern era fast growths in nanotechnology, in the field of electronics and electrical systems the capacitors with incredible performance are immediately required. At present, nanomaterials having a high dielectric constant and flexibility, but low dielectric loss, have attracted great consideration due to their potential presentation in many cutting-edge industries, including microelectronics, aerospace, and aviation[8-10]. In general, Iron (iii) Oxide (Fe_2O_3) own excellent flexibility and high breakdown strength,

Previous studies have shown that the polymeric composites, which were integrated with high thermal conductivity fillers, such as metal (Cu) [11], oxide(Al_2O_3)[12], aluminum nitride (AlN)[13], carbide(SiC)[14], and carbon nanotubes[15], can endow themselves with superior properties. For example, Cu-filled low-density polyethylene (LDPE) composites were studied by Luyt *et al*.[11] and they found that the thermal conductivity of the composites was 0.35 $W\,m^{-1}\,K^{-1}$ when the volume fraction of the Cu particles was 7.0 vol.%. Fang *et al*.[14] prepared different dimensional SiC particles to be filled into LDPE composites, and realized that the thermal conductivity of the composites was 0.37 $W\,m^{-1}\,K^{-1}$ at 10 vol.% SiC content. High thermal conductivity of the composites usually requires a high volume fraction of fillers, and provision of a low dielectric constant, which is not suitable for use for microelectronics. Additionally, most research has just focused on one single side of thermal conductivity or dielectric property of nanocomposites at room temperature. Few in-depth explorations of the cooperative effect of a large thermal conductivity and a high dielectric constant for polymer materials under broader temperature conditions have been investigated until now, and their influential mechanism is still uncertain. Beyond that, how to improve the thermal conductivity and the dielectric performance of composites at low filler loading is one of the key issues.

The external electric field could significantly influence the polymer's molecular arrangement and the conductive particles' distribution of the polymer composites, in the end the microstructure and macro-properties of the composites are influenced [16-17]. Hence, in this research, the electrical properties of Iron (iii) Oxide (Fe_2O_3) particles such as loss tangent, relative permittivity, relative loss and conductivity have been investigated at different frequencies at room temperature were investigated.

2. EXPERIMENTAL ANALYSIS

The nano Iron (iii) Oxide Nanopowder X-ray diffraction was conducted on a Philips Analytical XPERT-3 diffractometer using a Cu Kα radiation (λ = 1.54056 A°) with a MINIPROP detector and operating at 40 kV and 30 mA. X-ray diffraction patterns were recorded between 2θ = 5◦ and 109◦ with a step of 0.013◦ and a scan step time of 18.87 s by step. Identifier Diffraction software. Surface morphologies of the specimens were observed with a scanning electron microscope (SEM, JEOL JEC3000FC) in which coating time is 60 sec operating from 1kv to 5kv and using 70% inert gas. In the Raman spectroscopy the experiment time is 30sec, laser power is used 0.5% and the range is selected from 100-2000 cts using Renishaw model of Raman spectroscopy.

The dielectric measurements for the samples have been carried out with the dielectric cells in the form of parallel-plate capacitor. For unaligned, the dielectric cell has been prepared using indium tin oxide-coated glass plates, having surface resistance less than 1.0-1.5 ΩSq^{-1} The material has been filled in the cell at room temperature with the novo impedance analyser.

3. RESULT AND DISCUSSION

The figure 1 depicts the X-ray diffraction (Cu Kα radiation) spectrum of the nano Iron (iii) Oxide powder. The synthesized magnetic nanoparticles oxide shows good nanoparticles structure and are stable in hydrocarbon solvents against air oxidation. Figure 1 show the XRD patterns of Iron (iii) Oxide powder at room temperature. The nano- Iron (iii) Oxide powders are in amorphous structure. Its average particle size was 48.53 nm. That calculated through the Scherrer's formula $D=k\lambda/\beta\cos\theta$ [9] Scanning electron microscopy (SEM) micrograph of agglomerated nanocrystalline Iron (iii) Oxide particles produced. Scanning electron microscopy (SEM) images of Iron (iii) Oxide nanoparticles (figure 2, 3 & 4) indicating the homogeneous size, agglomeration of particles, with diameters ranging from 40 to 60 nm. The morphology of the prepared Iron (iii) Oxide nanoparticles was characterized by SEM images as shown in Figure 2-4. From images results, we can observe a large quantity of uniform nanoparticles (NPs) with average particle size of 40-60 nm.

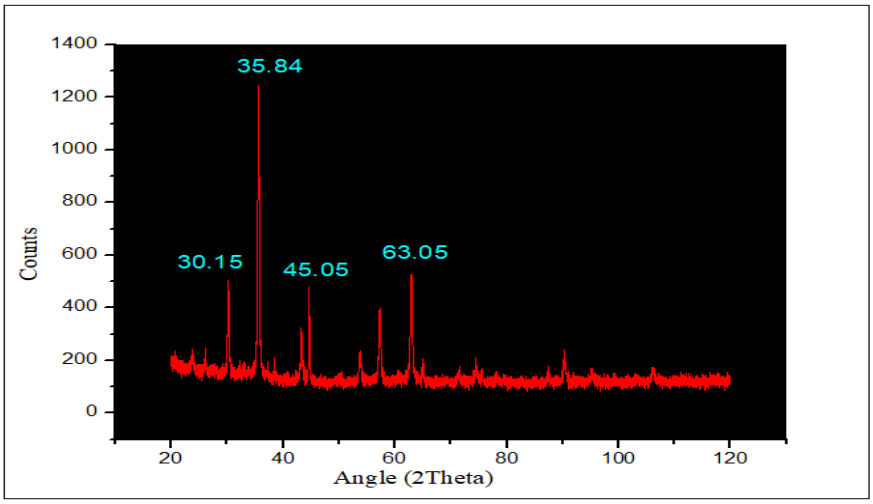

Figure 1 xrd pattern of Iron (iii) Oxide Nanopowder.

3.1. Morphological Analysis

The morphology of Iron (iii) Oxide Nanopowder was explored scanning electron microscope displayed in Figure 2 Iron (iii) Oxide Nanopowder.

These pictures display the formation of Iron (iii) Oxide Nanopowder. The pictures also exhibit the standardized particle size and specific range of diameters 30-40 nm.

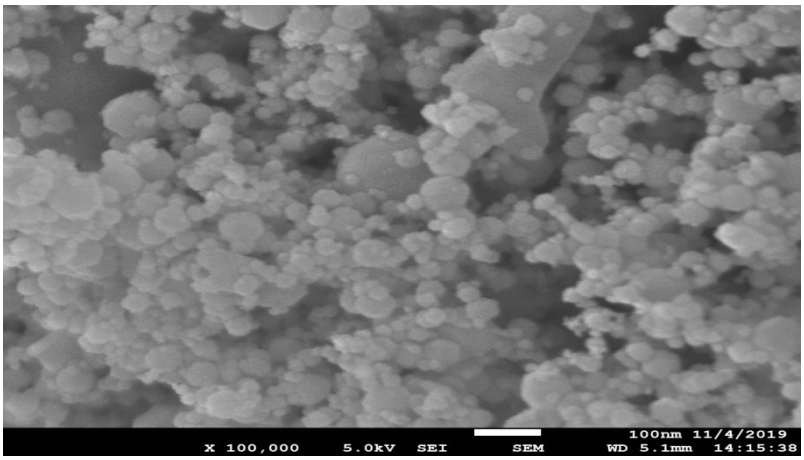

Figure 2 Scanning electron microscope photographs of Iron (iii) Oxide Nanopowder.

3.2. Raman Analysis

Figure 3 shows Raman spectra of Iron Oxide (iii) Nanopowder using a green laser with λ =785 nm. BN exhibits a characteristic peak occurs at ≈143, 289, 498 and 629 cm^{-1}. The intensity of the spectra is ~1500. Raman spectrograph display the regular peak. Raman spectra of ZnO confines the Iron Oxide (iii) Nanopowder.

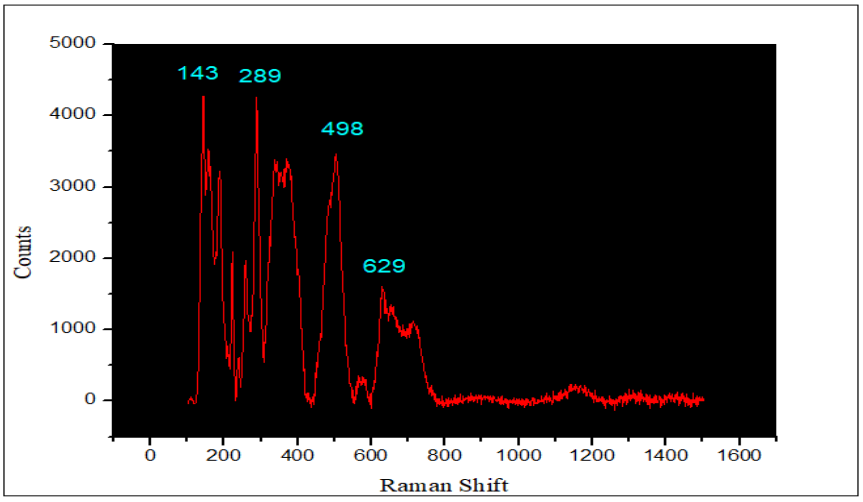

Figure 3 Raman shift (cm-1) vs. intensity of the Iron (iii) Oxide nanopowder at 28 ℃.

3.3. Electrical Analysis

The Electrical studies of sample were investigated by Novo impedance analyser α- type. The dependency of Electrical parameters (Electrical Conductivity and Dissipation Factor) on the frequency is given in the following table.

Table 1 Variation of Electrical Parameters viz. Frequency of the Iron (iii) Oxide nanopowder at Room Temperature 28 ºC.

Frequency (Hz)	Z (Ω)	Y $(Ω)^{-1}$	ε'	ε''	σ $(S\text{-}m^{-1})$	Tan δ
1 kHz	8.9×10^3	8.81×10^{-5}	1.09×10^3	1.40×10^3	1.24×10^{-4}	1.28
10 kHz	4.27×10^3	2.21×10^{-4}	1.25×10^2	3.55×10^2	3.1×10^{-4}	2.85
100 kHz	3.19×10^3	3.07×10^{-4}	9.64	4.75×10^1	4.31×10^{-4}	4.93
1 MHz	2.3×10^3	4.00×10^{-4}	2.67	6.25	5.62×10^{-4}	2.34
10 MHz	8.65×10^2	6.21×10^{-4}	1.54	0.97	8.72×10^{-4}	0.63

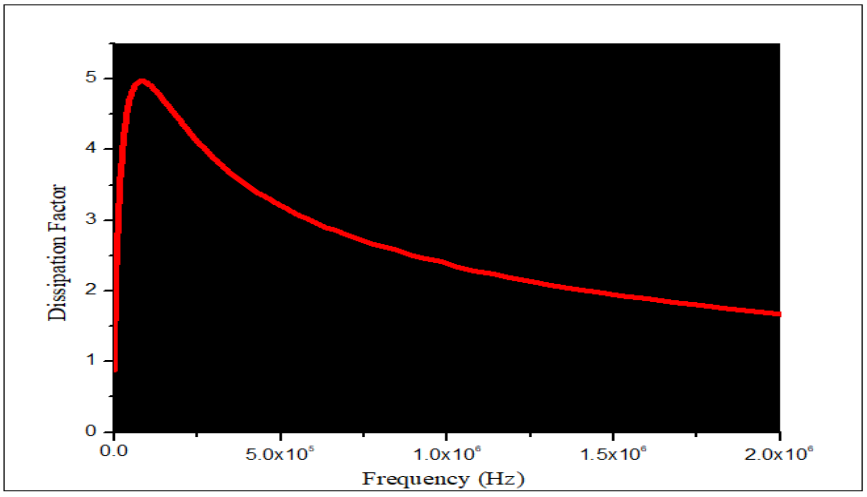

Figure 4 Dependency of Dissipation factor (Tan δ) on frequency (Hz) of Iron (iii) Oxide nanopowder at Temperature 28 ºC

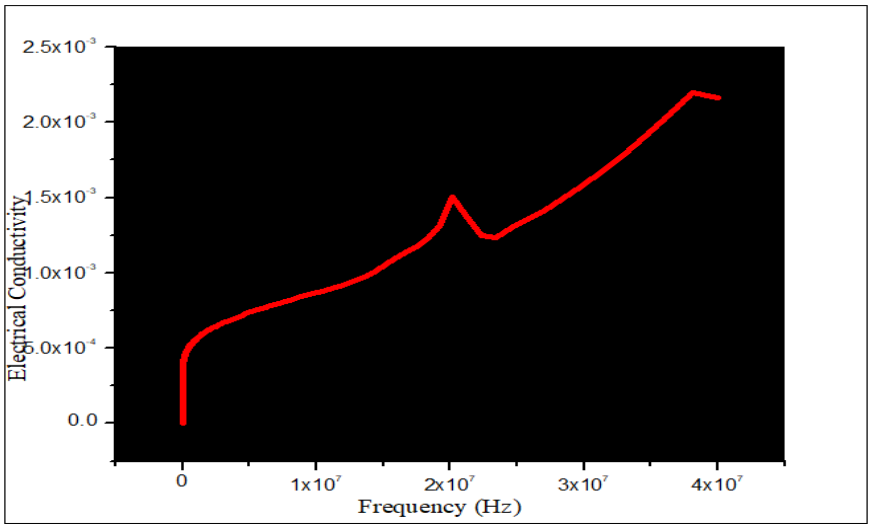

Figure 5 Dependency of electrical conductivity (σ) on frequency (Hz) of Iron (iii) Oxide nanopowder at Temperature 28 ºC

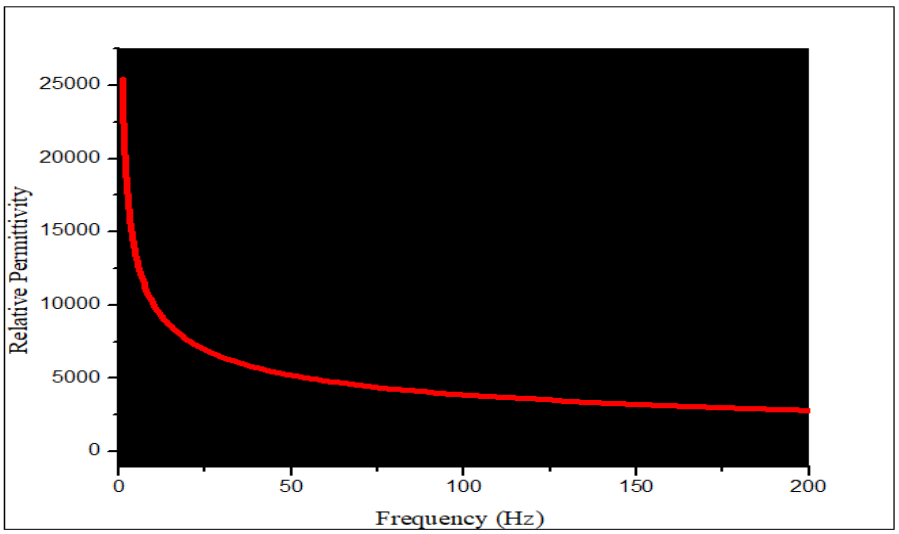

Figure 6 Dependency of relative permittivity (ε') on frequency (Hz) of Iron (iii) Oxide nanopowder at Temperature 28 ºC

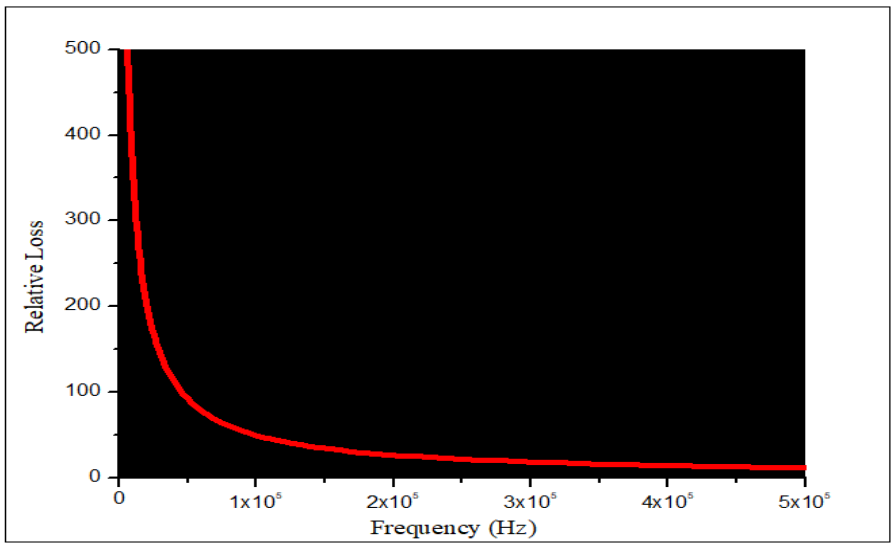

Figure 7 Dependency of relative loss (ε") on frequency (Hz) of Iron (iii) Oxide nanopowder at Temperature 28 ºC

4. CONCLUSION

This study has described that at room temperature the structural and electrical study of Iron (iii) Oxide (Fe_2O_3) has done. It is found that the Iron (iii) Oxide (Fe_2O_3) with homogeneous size of 30-40 nm, shape distribution agglomeration of particles, with diameters extending from 30 to 40 nm have been characterized by SEM, XRD and RAMAN SPECTROSCOPY it is found that the Iron (iii) Oxide (Fe_2O_3) has crystalline structure and homogenenous size of the particles within the nanoscale. In addition, Electrical parameters of Iron (iii) Oxide (Fe_2O_3) such as dissipation factor (Tan δ), and electrical conductivity (σ) with the frequency analysed by Novo Impedance Analyser and found that conductivity [σ] varies from 1.24×10^{-4} ($S\text{-}m^{-1}$) to 8.72×10^{-4} ($S\text{-}m^{-1}$) with frequency 1 KHz to 10 MHz, while the Loss Tangent Varies from 1.28 to 0.63 with the same frequency range. This variation was obtained owing to drop in the size of Iron (iii) Oxide (Fe_2O_3) Nano Powder.

On the basis of this analysis the Iron (iii) Oxide (Fe_2O_3) Nanopowder can be used as dielectric material.

ACKNOWLEDGEMENTS

We are thankful to Director Birbal Shahni Institute of Paleoscience, Lucknow and Coordinator Centre of Material Science, University of Allahabad, Prayagraj for the infrastructure.

CONFLICT OF INTEREST

This Study does not have any conflict of interest.

REFERENCES

[1] Y.W. Jun, J.W. Seo, J. Cheon, Acc. Chem. Res. 41(2008) 179-189. https://doi.org/10.1021/ar700121f

[2] L. R. Bickford, Phys. Rev. 78(1950) 449. https://doi.org/10.1103/PhysRev.78.449

[3] M. Jeun, S. Lee, J. K. Kang, A. T. Tomitaka, K. W. Kang, Y. I. Kim, Y. Takemura, K.-W. Chung, J. Kwak, S. Bae, Appl. Phys. Lett. 100, (2012) 092406. https://doi.org/10.1063/1.3689751

[4] S. Guo, D. Li, L. Zhang, J. Li, E. Wang, Biomaterials. 30(2009) 1881. https://doi.org/10.1016/j.biomaterials.2008.12.042

[5] R. Hao, R. Xing, Z. Xu, Y. Hou, S. Gao, S. Sun, Adv. Mater. 22(2010) 2729. https://doi.org/10.1002/adma.201000260

[6] A. G. Roca, D. Carmona, N. Miguel-Sancho, O. Bomati-Miguel, F. Balas, C. Piquer, J. Santamaría, Nanotechnology 23(2012) 155603. https://doi.org/10.1088/0957-4484/23/15/155603

[7] J. Llandro, J. J. Palfreyman, A. Ionescu, and C. H. W. Barnes, Med. Biol. Eng. Comput. 48(2010) 977. https://doi.org/10.1007/s11517-010-0649-3

[8] P. O. Rocío, F. Antonio, T. J. Marks, Chem. Rev. 110(2010) 205–239.

[9] Q. G. Chi, et al. J. Alloy Compd. 559(2013) 45–48.

[10] A. S. Luyt, J. A. Moldefi, H. Krump, Polym. Degrad. Stabil. 91(2006) 1629–1636.

[11] Y. Yang, J. L. He, G. N. Wu, J. Hu, Sci. Rep 5(2015) 16986.

[12] C. Min, D. Yu, J. Cao, G. Wang, L. Feng, Carbon 55(2013) 116–125.

[13] F. Ren, P. G. Ren, Y. Y. Di, D. M. Chen, G. G. Liu, Polym. Plast. Technol 50(2011) 791–796.

[14] J. L. Zeng, et al. J. Therm. Anal. Calorim. 95(2009) 507–512.

[15] C. Yuan, et al. ACS Appl. Mater. Interfaces 7(2015) 13000–13006.

[16] W. P. Li, L. J. Yu, Y. J. Zhu, D. Y. Hua, J. Phys. Chem. C 114(2010) 14004–14007.

[17] Q. G. Chi, et al. J. Mater. Chem. C 4(2016) 8179–8188.